fermentation

MDPI

Article

Particle Size Effect on Anaerobic Digestion of Fruit and Vegetable Waste

José Vian [1,2], Alejandra Velasco-Pérez [2,*], Rocío Solar-González [3], Tania García-Herrera [2], Hector Puebla [4] and Guadalupe Vivar-Vera [2]

[1] Universidad Politécnica de Huatusco, Unidad Chocamán, Chocamán 94160, Mexico; ibvianperez@gmail.com
[2] Facultad de Ciencias Químicas, Universidad Veracruzana, Región Orizaba-Córdoba, Orizaba 94340, Mexico; tangarcia@uv.mx (T.G.-H.); gvivar@uv.mx (G.V.-V.)
[3] Universidad del Istmo Campus Tehuantepec, Sto. Domingo Tehuantepec, Oaxaca 70760, Mexico; solgr@sandunga.unistmo.edu.mx
[4] Departamento de Energía, Universidad Autónoma Metropolitana Azcapotzalco, Ciudad de México 02128, Mexico; hpuebla@azc.uam.mx
* Correspondence: alvelasco@uv.mx; Tel.: +52-2727240120

Abstract: During the anaerobic digestion (AD) of fruit and vegetable waste (FVW), excessive particle size reduction can lead to the overproduction and inhibition of methanogenic microorganisms. This paper presents an in-depth analysis through experimental assays, modeling, and response surface analysis of the effect of particle size on methane production. A simple model was proposed considering the inhibition of the growth of methanogenic microorganisms and surface-based hydrolysis kinetics. The model parameters were estimated using experimental data from batch systems fed with FVW of varying particle sizes (ranging from 1.8 to 1000 µm). Response surface methodology establishes a statistical model for estimating methane production based on particle size and concentration. Numerical and statistical analyses were conducted using Matlab R2024a and Minitab 24 software. A model with an R^2 of 0.89 was obtained, which determined an optimal concentration of 8.2 kg·m^{-3} and a particle size of 742.3 µm, yielding a methane production of 303.3 m^3·kg^{-1} VS, similar to the experimentally obtained range of 300.95 to 316.7 m^3·kg^{-1} VS.

Keywords: anaerobic digestion; fruit and vegetable waste; particle size; mathematical model; surface response methodology

check for updates

Citation: Vian, J.; Velasco-Pérez, A.; Solar-González, R.; García-Herrera, T.; Puebla, H.; Vivar-Vera, G. Particle Size Effect on Anaerobic Digestion of Fruit and Vegetable Waste. *Fermentation* **2024**, *10*, 485. https://doi.org/10.3390/fermentation10090485

Academic Editor: Giulia Bozzano

Received: 26 July 2024
Revised: 5 September 2024
Accepted: 14 September 2024
Published: 18 September 2024

Copyright: © 2024 by the authors. Licensee MDPI, Basel, Switzerland. This article is an open access article distributed under the terms and conditions of the Creative Commons Attribution (CC BY) license (https://creativecommons.org/licenses/by/4.0/).

1. Introduction

The inadequate disposal and underutilization of municipal solid waste is a social and environmental issue at present. A matter of particular concern is FVW, as it accounts for 60% of globally lost or wasted food [1,2]. Disposal in landfills or open dumps leads to the release of greenhouse gases, leachate filtration into the subsoil, and the creation of habitats for harmful fauna and infectious agents [3,4]. An alternative to this problem is the stabilization of waste through anaerobic digestion (AD). This technology offers advantages such as low energy requirements, energy recovery through methane generation, and the production of digestate that can be used for agricultural purposes [5,6].

The AD process converts organic matter into methane through four stages: disintegration-hydrolysis, acidogenesis, acetogenesis, and methanogenesis. These stages are carried out simultaneously by distinct microbial consortia [7]. When designing anaerobic technology, the engineering objective is to achieve high methane productivity and substantial solid removal efficiencies while operating the reactors with short retention times [8]. This is accomplished by ensuring the balanced growth of different microbial populations, so the products of one stage are consumed at the same rate in the subsequent stage without the accumulation of intermediates [9]. The stable performance of AD depends on physicochemical factors

such as pH and temperature, operational conditions including hydrodynamics, and solid concentration, but primarily on the characteristics of the feedstock [5,9–11].

Regarding FVW, two aspects related to the nature of the waste need to be analyzed. Firstly, it is widely accepted that hydrolysis is the limiting stage in the AD of particulate matter [8,12]. This is because hydrolytic enzymes adhere to the surface of the waste, initiating the degradation of the solid matrix to release soluble compounds [13]. Consequently, reducing the particle size can increase the overall reaction rate by enhancing the available surface area of the waste [14]. For instance, decreasing the particle size of food waste by 58% increased waste solubilization from 28% to 40% over the same period [15]. However, in FVW, 56% and 75% of volatile solids (VS) comprise sugars and hemicellulose, resulting in biodegradability exceeding 72% [16]. These compounds are rapidly solubilized and metabolized by acidogenic microorganisms, producing volatile fatty acids (VFA). Therefore, when the organic loading rate (OLR) exceeds 3.5 kg $VS \cdot m^{-3} \cdot d^{-1}$, VFA can accumulate, decreasing the pH and inhibiting the growth of the methanogenic population [12,15,17]. Additionally, although physical and mechanical pre-treatments can improve the AD of FVW by altering the substrate structure and reducing particle size, smaller particles can result in higher economic costs and increased VFA buildup [18,19]. Hence, it is crucial to identify the dependencies of FVW concentration and particle size on methane production and the overall performance of AD.

A compelling approach to analyzing AD performance is the exploration of different operational scenarios using process modeling and simulation. This approach significantly improves the understanding of the process while optimizing time, resources, and effort [20,21]. Several mathematical models have been developed to achieve this goal. Early models were a simplification of the AD process that considered only the methanogenic stage with inhibition due to the accumulation of VFA [22]. Later, more complex models were developed, incorporating more specific microbial populations and additional inhibition phenomena, such as ammonia inhibition of methanogens [23], transport phenomena, and feedstock composition [24]. In 2002, the Anaerobic Digestion Model No. 1 (ADM1) was published, encompassing the fundamental biochemical pathways from hydrolysis to acetoclastic and hydrogenotrophic methanogenesis. The model consists of 19 differential and 12 algebraic equations, describing 24 state variables [25]. Owing to its detailed and comprehensive structure, the ADM1 model has served as a platform for precise modeling and simulation of anaerobic digestion across various feedstocks and systems [26].

However, implementing the ADM1 model requires a thorough characterization of substrates and model parameters, and to ensure the accuracy and sensitivity of the model, rigorous calibration and validation efforts are imperative [27]. Then, precise measurement data on substrate composition, intermediates, and biogas composition are required [28]. For these reasons, simplified structure models offer considerable advantages in applicability, requiring the estimation of fewer parameters, thereby facilitating other engineering tasks such as design, optimization, and process control [29].

This paper presents an in-depth, model-based analysis of the effect of particle size and substrate concentration on anaerobic digestion (AD) performance, specifically focusing on methane production. To achieve this, experimental assays of AD using food and vegetable waste (FVW) were conducted in batch reactors. Subsequently, a simplified model was proposed, integrating microbial groups into two populations: acidogenic and methanogenic microorganisms. By incorporating a surface-based kinetic constant for hydrolysis into the model, it was possible to analyze the effect of feedstock particle size on AD performance under varying organic concentrations, thereby identifying viable operating conditions for treating this type of waste. Additionally, a statistical model was introduced to estimate methane production based on particle size, which was then used to determine the maximum potential methane yield.

2. Materials and Methods

2.1. Batch Assays of Anaerobic Digestion of Fruit and Vegetable Waste

The FVW was obtained from a fruit cocktail and salad establishment in the municipality of Ecatepec, State of Mexico. The FVW mixture consisted of 6% beetroot, 5% radish, 28% jicama, 2% lemon, 38% cucumber, 6% pineapple, and 16% carrot. Physicochemical characterization was performed by determining pH [30] and the contents of moisture, total solids (TS) and VS [31]. The nitrogen [32] and chemical oxygen demand (COD) [24] content was quantified in an FVW suspension with a concentration of 1 kg TS·m^3. The suspension was prepared as follows: a portion of the food and vegetable waste (FVW) was dried, ground, and sieved to obtain particles smaller than 500 µm, which were then resuspended in distilled water. The C/N ratio was calculated by multiplying the COD to nitrogen content ratio by 0.35 [33].

The inoculum was anaerobic granular sludge from an industrial UASB reactor. The concentration of volatile suspended solids (VSS) in the sludge was 0.0631 kg VSS·kg$^{-1}_{\text{wetsludge}}$, with a specific methanogenic activity (SMA) of 1.23 ± 0.36 kg COD_{CH_4}·kg^{-1} VSS·d^{-1}.

AD of FVW was carried out in batch reactors with a total volume of 120 mL (effective volume of 80 mL) inoculated with granular sludge. The concentration of inoculum and substrate was 2.5 kg VSS·m^{-3} and 4 kg COD·m^{-3}, respectively. Three experiments were conducted in triplicate, varying the particle size of the fed FVW between each. The reactor volume was completed with revised anaerobic mineral medium (RAMM) without a carbon source [34]. The pH was adjusted to 7 with KOH, and 0.5 kg of $NaHCO_3$ was added per kg of COD to improve buffer capacity in the system. The reactors were sealed and placed in an incubator at 35°. The generated methane was quantified by displacing a 1.5% KOH solution in a Mariotte-type device. Due to the small volume of the reactors, it was not possible to monitor the pH dynamics throughout the experiments; however, the pH of the reaction medium was measured at the end of each experiment [30]. An additional experiment was performed, subjecting the FVW to AD without inoculum to investigate the substrate consumption by its autochthonous microorganisms.

The particle sizes of the FVW in the different experiments were in the ranges $1.8 - 500$ µm (PS1), $500 - 1000$ µm (PS2), and > 1000 µm (PS3). For the no-inoculum experiment, the PS2 particle size range was used. To obtain samples with these particle sizes, 0.2 kg of FVW was triturated in a blender with 200 mL of distilled water. The mixture was sieved consecutively using sieves with openings of 1000 and 500 µm. PS3 particles did not pass through the first sieve, and PS2 particles were retained in the second sieve. These particles were washed with distilled water until a concentration < 0.05 kg COD·m^{-3} was reached in the wash water to remove the soluble fraction of the FVW. The fraction that passed through the 500 µm sieve was centrifuged at 3500 rpm for 15 min. The sediment was washed with 270 mL of water, thus obtaining the PS1 particles.

2.2. Model Description

The dynamic mathematical model proposed has been derived from previous works where the most important aspects of the anaerobic digestion of FVW have been modeled. Key factors include the particle size effect [13,35] and process inhibition due to the accumulation of volatile fatty acids [24,36]. The model considers only the hydrolysis, acidogenesis, and methanogenesis phases, which can be represented by the following reactions:

$$S_p \rightarrow S_s \quad (1)$$

$$S_s \rightarrow X_a + S_a \quad (2)$$

$$S_a \rightarrow X_m + M \quad (3)$$

where S_p denotes the particulate matter, i.e., the FVW; S_s represents the soluble substrate such as sugars, amino acids, and short-chain fatty acids; S_a refers to VFA; X_a denotes

acidogenic microorganisms; X_m represents methanogenic microorganisms; and M is the product methane.

2.2.1. Hydrolysis

To model the hydrolysis of S_p, it is assumed that all substrate particles are spherical in shape and that their surface undergoes uniform degradation over time due to enzymatic action. Therefore, the hydrolysis rate is described using Equation (4), derived by Esposito et al. [35].

$$r_{hyd} = -K_{sbk} \cdot a^* \cdot S_p \tag{4}$$

where r_{hyd} is the hydrolysis rate ($kg \cdot m^{-3} \cdot d^{-1}$), K_{sbk} is the surface-based hydrolysis rate constant $\left(kg \cdot m^{-2} \cdot d^{-1}\right)$, and a^* is the ratio between the surface area and the mass of the particles ($m^2 \cdot kg^{-1}$).

Considering spherical particles, a^* varies according to the following expressions:

$$a^* = \frac{A}{m} = \frac{4\pi R^2}{\rho \frac{4}{3} \pi R^3} = \frac{3}{\rho R} \tag{5}$$

$$R = R_0 - K_{sbk} \frac{\rho}{t} \tag{6}$$

where A is the surface area (m^2), m is the particle mass (kg), ρ $\left(kg \cdot m^{-3}\right)$, R (m), and R_0 (m) refer to the density, radius, and initial radius of the particles, respectively, and t is the time of process (d).

Then, the mass balance in a discontinuous reactor is expressed as follows:

$$\frac{dS_p}{dt} = -K_{sbk} \cdot a^* \cdot S_p \tag{7}$$

2.2.2. Acidogenesis and Methanogenesis

The stages of acidogenesis and methanogenesis are described through the growth of microbial populations since these are intracellular processes. The specific growth rate of acidogenic bacteria has been described using the Monod kinetic model [37]:

$$\mu_a = \frac{\mu_{max,a} \, S_s}{K_{s,a} + S_s} \tag{8}$$

where μ_a represents the specific growth rate (d^{-1}), $\mu_{max,a}$ is the maximum specific growth rate (d^{-1}), and $K_{s,a}$ is the saturation constant $(kg \cdot m^{-3})$ for acidogenic bacteria. For the mathematical representation of the methanogenic stage, the phenomenon of inhibition of microbial growth due to the accumulation of substrate (VFA) was considered. Therefore, the specific growth rate was described with the Haldane kinetic model [38]:

$$\mu_m = \frac{\mu_{max,m} \, S_a}{K_{s,m} + S_a + \frac{S_a^2}{K_{im}}} \tag{9}$$

where $\mu_{max,m}$ is the maximum specific growth rate (d^{-1}), $K_{s,m}$ is the saturation constant $(kg \cdot m^{-3})$ for methanogens, and K_{im} is the inhibition constant by VFAs $(kg \cdot m^{-3})$.

The process of cell death is also considered in the model. It is represented by first-order kinetics characterized by constants k_{da} and k_{dm} (d^{-1}) for acidogenic and methanogenic microorganisms, respectively.

To establish the mass balance of soluble material and biomass, it is assumed that the inoculum is constantly enriched with the residues entering the reactor, and dead

microorganisms are reincorporated as soluble matter. Thus, the balance equations for microorganisms and soluble substrates are as follows:

$$\frac{dS_s}{dt} = K_{sbk} a^* S_p - \frac{1}{Y_{xa,s}} \mu_a X_a + k_{da} X_a + k_{dm} X_m \quad (10)$$

$$\frac{dX_a}{dt} = \mu_a X_a - k_{da} X_a \quad (11)$$

$$\frac{dS_a}{dt} = Y_{a,xa} \mu_a X_a - \frac{1}{Y_{xm,a}} \mu_m X_m \quad (12)$$

$$\frac{dX_m}{dt} = \mu_m X_m - k_{dm} X_m \quad (13)$$

$$\frac{dM}{dt} = Y_{M,xm} \mu_m X_m \quad (14)$$

where $Y_{xa,s}$ and $Y_{a,xa}$ are the biomass/substrate and product/biomass yield coefficients for acidogens $\left(\text{kg}\cdot\text{kg}^{-1}\right)$ and $Y_{xm,a}$ and $Y_{M,xm}$ are the same types of yield coefficients but for methanogens.

2.2.3. Parameter Estimation

The kinetic parameters and yield coefficients were taken from the literature and are presented in Table 1. The parameters estimated were the constants K_{sbk} and K_{im} using accumulated methane data from batch tests of FVW AD (PS1 Section 2.1). The estimation was carried out by minimizing the squared error between the experimental data and the model response, as follows:

$$J(\phi) = min \sum_{t=1}^{N} \left[v_{exp}(t) - v_{sim}(t, \theta) \right]^2 \quad (15)$$

where J denotes the objective function, $v_{exp}(t)$ refers to the vector of experimental data, and $v_{sim}(t, \theta)$ is the vector of simulated data as a function of time and model parameters θ. An integration program was used to solve the system of differential equations using the fourth-order Runge–Kutta method to calculate the model predictions. For parameter estimation, the model was evaluated with $D = 0$ since the data originated from batch tests. The optimization problem was solved using the interior-point algorithm through the fmincon function in Matlab R2024a software with a tolerance value $< 1.02 \times 10^{-6}$.

Table 1. Kinetic parameters and yield coefficients for model solution.

Parameter	Value (Units)	Reference	Parameter	Value (Units)	Reference
$\mu_{max,a}$	1.5 (d^{-1})	[39]	$Y_{xa,s}$	0.2 $(\text{kg}\cdot\text{kg}^{-1})$	[23]
$K_{s,a}$	0.26 $(\text{kg}\cdot\text{m}^{-3})$	[39]	$Y_{a,xa}$	2.45 $(\text{kg}\cdot\text{kg}^{-1})$	[23]
$\mu_{max,m}$	0.138 (d^{-1})	[39]	$Y_{xm,a}$	0.06 $(\text{kg}\cdot\text{kg}^{-1})$	[23]
$K_{s,m}$	0.003 $(\text{kg}\cdot\text{m}^{-3})$	[39]	$Y_{M,xm}$ *	18.26 $(\text{m}^3\cdot\text{kg}^{-1})$	[23]
K_{im}	0.3 $(\text{kg}\cdot\text{m}^{-3})$	[39]			

* At 35 °C.

For the death cell kinetic constants, it is assumed that k_{da} and k_{dm} are 5% and 1%, respectively, of the specific growth rate of acidogenic and methanogenic microorganisms [24].

In addition, to determine the concentration of microorganisms in the FVW, the initial concentration of acidogens (X_a) and methanogens (X_m) were estimated using accumulated methane data from the no-inoculum experiment, and the problem presented in Equation (15) was solved.

2.2.4. Sensitivity Analysis

To determine the parameters that significantly affect the model response, a parametric sensitivity analysis was performed. The sensitivity function was calculated using the relative local sensitivity method. Sensitivities were estimated through variations in the state variables under perturbations in the model parameters. The numerical solution for the problem was performed using a finite differences approximation based on Equation (16) [40].

$$S_{ij} = \frac{\partial x_i / x_i}{\partial \theta_j / \theta_j} \approx \frac{\left(x_i\left(t, \theta_j + \delta\theta_j\right) - x_i\left(t, \theta_j\right)\right) / x_i\left(t, \theta_j\right)}{\delta\theta_j / \theta_j} \quad (16)$$

where S_{ij} is the normalized sensitivity value of the i-th state variable (S_s, S_a, and M) with respect to the j-th parameter. Starting parameter values and the values estimated for K_{sbk} and K_{im} are reported in Table 1. The perturbation factor δ was set to 0.1 (10%) for all calculations.

2.2.5. Model Validation and Simulation in Continuous Regime

To validate the model, its output was compared to the accumulated methane data from the DA tests with particles of $500 - 1000$ µm and > 1000 µm (PS2 and PS3, Section 2.1). To evaluate the goodness of fit, the coefficient of determination $\left(R^2\right)$ was calculated. R^2 was used because it indicates the percentage of variability in the dependent variable (output) that can be explained by the independent variable (input). The value of R^2 is calculated according to Equation (17) and ranges from 0 to 1. When its value is closer to 1, the reliability of the model can be assumed [41].

$$R^2 = 1 - \frac{SS_{res}}{SS_{tot}} \quad (17)$$

where SS_{res} refers to the sum of the squared differences between the observed data and the predicted values, and SS_{tot} indicates the sum of the squared differences between the observed data and their mean.

Simulations of the model were carried out to investigate the combined effect of concentration and particle size of FVW on methane production in a discontinuous manner. To identify the effects and to determine the best operational region, the surface response methodology was applied to simulated data according to the central composite design of experiments without replicates and setting the significance (α) to 0.1, or in other words, a confidence level of 0.9 [42]. The statistical analysis was carried out using the Minitab 22 software. The experimental design is presented in Table 2; for each factor, two levels were selected, and the information was complemented with four external points and one central point.

Table 2. Central composite design for the surface response model.

	Concentration $\left(\mathbf{kg \cdot m^{-3}}\right)$				
Particle Size (µm)	**5.58**	**6**	**7**	**8**	**8.41**
125.74					
250.00					
550.00	*				
850.00					
947.26					

* Shaded cells correspond to evaluated conditions.

The levels were identified by screening the accumulated methane simulated, varying the particle size from 100 to 1000 µm and the concentration from 4 to 10 $kg \cdot m^{-3}$.

3. Results and Discussion

3.1. Fruit and Vegetable Waste Characterization and Methane Production

The physicochemical characteristics of the FVW sample used in this work are presented in Table 3. The FVW exhibits a pH and an organic matter content similar to values reported in other studies, with a moisture content > 80% and a VS percentage of 6–18% [16,43,44]. It can also be observed that, in terms of nutrient proportion, denoted by the C/N ratio, the FVW sample presents a value of 14.46, which is below the optimal range of 20–30. This implies that caution must be exercised when applying high organic loads, as there may be ammonia accumulation and inhibition of methanogenic activity [45].

Table 3. Physicochemical characterization of fruit and vegetable waste.

Parameter	Units	Value
pH	-	5
Moisture	%	91.5
TS	$kg \cdot kg^{-1}$ waste	0.085
VS	$kg \cdot kg^{-1}$ waste	0.074
COD	$kg \cdot kg^{-1}$ TS	0.813
Nitrogen	$kg \cdot kg^{-1}$ TS	0.019
C/N	-	14.76

Regarding the methane yield from the FVW mixture at different particle sizes, it can be observed in Figure 1 that a lower yield was obtained for PS1 (185 $m^3 \cdot kg^{-1}$ VS) compared with PS2 (316.7 $m^3 \cdot kg^{-1}$ VS) and PS3 (300.95 $m^3 \cdot kg^{-1}$ VS). This can be attributed to an inhibition phenomenon due to the accumulation of intermediates, which is consistent with the findings of Izumi et al. [15], who observed inhibition of methane production in the AD of food waste with a particle size of 393 µm. This premise is also supported by the pH values observed at the end of the experiments. Figure 1 shows that the pH for PS2 and PS3 was 7.55 and 7.98, respectively, while for PS1, it was 5.29, a value below the optimal pH range for methanogenesis (6.8–7.2) [5], which is also indicative of VFA accumulation [12,40,41]. The methane yield for the non-inhibited assays falls within the range reported in the literature review on the AD of FVW by Ji et al. [44], which presents yields from 190 to 473 $m^3 \cdot kg^{-1}$ VS, with the lowest value corresponding to the digestion of cauliflower leaves (rich in lignocellulosic material) and the highest value for the digestion of lemon waste (with a high sugar content). It was also observed that for the no-inoculum experiment (PS2*), a yield of 81 $m^3 \cdot kg^{-1}$ VS was obtained, which is 25% of the yield obtained for FVW digestion in the same particle size range (PS2) but with inoculum. This can be attributed to the deficit of exoenzymes due to the lack of inoculum, which causes slower substrate hydrolysis. Therefore, the decrease in methane yield compared to PS2 is not a consequence of VFA accumulation, as the pH of the medium at the end of the experiment was close to neutrality (pH = 6.75), as shown in Figure 1.

3.2. Parameter Estimation and Validation

The parameter values that minimized the square error between the model response and the observed data of the AD of FVW were $K_{sbk} = 0.0849\ kg \cdot m^{-2} \cdot d^{-1}$ and $K_{im} = 0.0642\ kg \cdot m^{-3}$. Figure 2a illustrates the experimental and simulated AD dynamics of the FVW in the assays conducted for parametric estimation. The determination coefficient obtained was $R^2 = 0.9301$, indicating that the model is suitable for mathematical process description using optimized parameters [41].

The estimated value for K_{im} is close to 0.04 and 0.059 $kg \cdot m^3$, which are the constants of inhibition for methanogenic microorganism growth reported in two-population models [39]. The value of K_{sbk} is in agreement with the literature too. For example, Sanders et al. [27] reported values of 0.0096 and 0.0108 $kg \cdot m^{-2} \cdot d^{-1}$ for the hydrolysis of potato starch with a particle size of 17 and 46 µm. Differences in values can be attributed to the structure

and homogeneity of the starch composition. Alternatively, Vigueras-Carmona et al. [46] found hydrolysis constant values ranging from 0.28×10^{-3} to 0.47×10^{-3} kg·m^{-2}·d^{-1} for residual sludge. These values denote a lower hydrolysis rate due to the recalcitrant nature of the exopolymers and the cell wall present in the sludge. Therefore, the estimated value of K_{sbk} is adequate for use, offering a good fit to experimental data and holding biochemical and physical significance. It can be assumed that the model is valid, as the R^2 coefficient obtained for assays with PS2 and PS3 was close to 1 (Figure 2c,d), indicating that the model explains the variability in the data and provides an adequate fit [41].

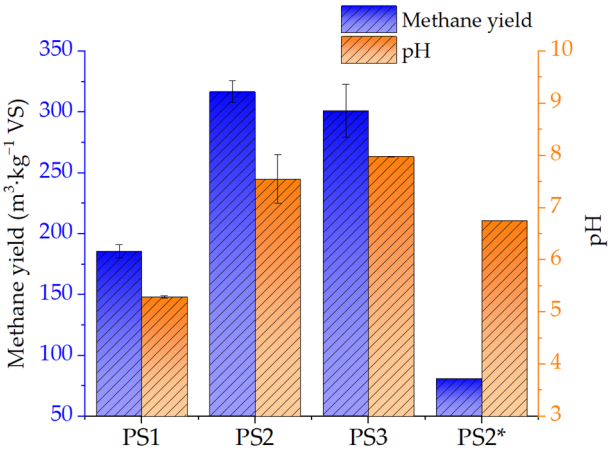


Figure 1. Methane yield and final pH from the AD of FVW with particle sizes of 1.8–500 µm (PS1), 500–1000 µm (PS2), and >1000 µm (PS3). The mean and standard deviations of the three replicates for each experiment are shown. PS2* refers to the no-inoculum experiment.

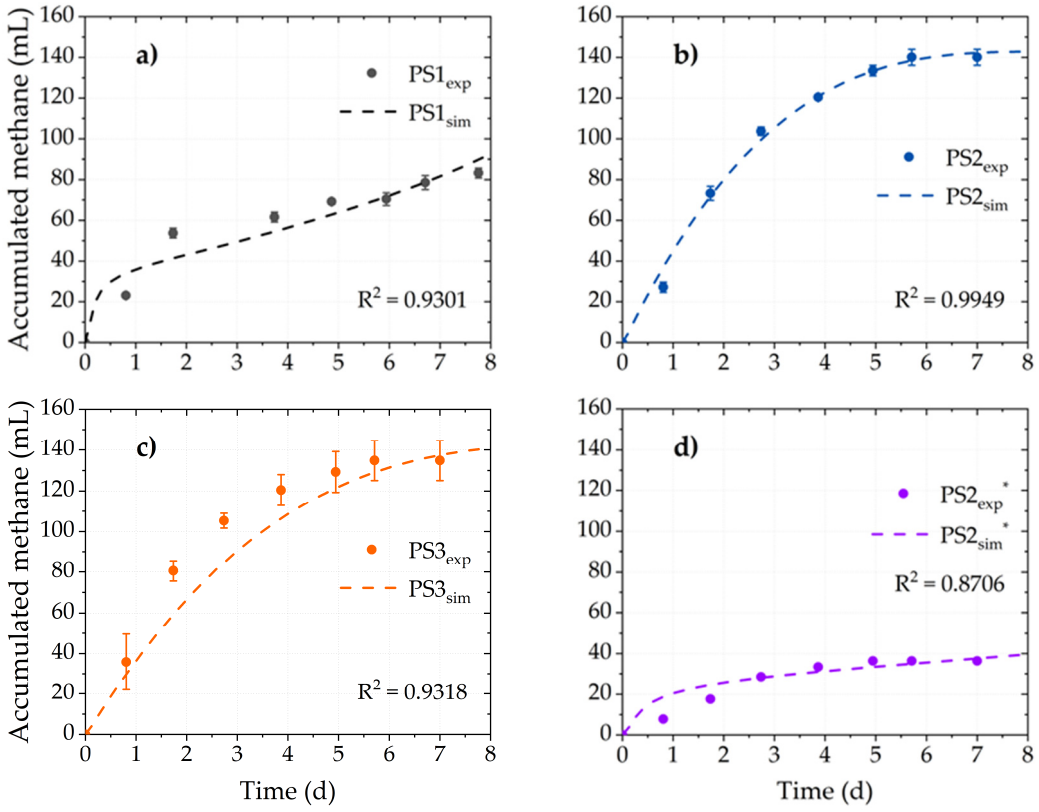


Figure 2. Experimental and simulated data of cumulative methane production from the anaerobic digestion of fruit and vegetable waste with different particle sizes: (**a**) 1.8–500 µm, (**b**) 500–1000 µm, (**c**) >1000 µm, and (**d**) 500–1000 µm without inoculum.

In the initial autochthonous biomass concentration estimation, values of 0.5074 and 0.2613 kg·m^{-3} were obtained for X_a and X_m with an R^2 coefficient equal to 0.8706 (Figure 2d). This means that acidogenic and methanogenic microorganisms constitute 66% and 34% of the microbial biomass in the FVW, respectively. This is consistent with another analysis where it was determined that the methanogenic population represents 35% of the biomass. The remaining 65% corresponds to acetogens and sugar, proteins, and long-chain fatty acid consumers. The importance of these values lies in their use as inputs for the model for future applications on continuous regimen simulation.

3.3. Sensitivity Analysis

The resulting normalized local sensitivity values of soluble substrate, VFA, and methane to the 10 parameters shown in Figure 3. It can be observed (Figure 3a–f) that kinetic parameters K_{sbk}, $\mu_{max,a}$, K_{sa}, $\mu_{max,m}$, K_{sm}, and K_{im} exhibit sensitivity before six days, while after this period the sensitivity is zero. Therefore, small variations in these parameters can influence the model output within this simulation time frame. This observation aligns with experimental results, as approximately 95% of the substrate is consumed by the sixth day, thus defining this day as the boundary of the dynamic phase of the process. In the simulation context, the transient phase is from day zero to day six, beyond which the model output remains virtually constant. The oscillations observed in the same figures are attributed to the nonlinearity of the model or the interrelation (recirculation) of the state variables of the system [47], especially when considering that the model structure accounts for cell death and its reintegration into the system as a fraction of S_s, in a cycle where this material is used for microbial growth but later returns. This effect is more pronounced for acidogenic bacteria, which have a higher specific growth rate than archaeal methanogens, making the phenomenon (recirculation) less intense in the dynamics of VFA (sensitivity represented with a blue dash in Figure 3).

Figure 3g–j illustrates the effect of perturbation of stoichiometric parameters (Y_{xas}, $Y_{a,xa}$, $Y_{xm,a}$, and $Y_{M,xm}$) on S_s, S_a, and M. In this case, it is observed that the effect of the parameters is significant throughout the entire process, reaching its maximum towards the end. Variations in these parameters significantly affect the model output regarding methane production. Proper calibration would allow for effective representation of the AD of various types of waste with two population models, noting that in the case of FVW, the methane yield spans a wide range of values (190–473 m^3·kg^{-1} VS) [44].

3.4. Effect of Particle Size and Substrate Concentration

In Figure 4, the simulation results of the process at different particle sizes and concentrations are shown. For the analysis of the process dynamics, the vertical line at time 6 in Figure 4 is used as a reference. This is because, for the AD of substrates rich in carbohydrates like FVW, 80% of methane production is achieved within four days of digestion [48], whereas, in this study, it was achieved in 6 days for the assays PS1 and PS2 (without inhibition). Therefore, process inhibition can be visualized as less than 80% methane production after 6 days. It can be observed that the accumulated methane curve for a particle size of 50 µm has a lower slope than that of 250 µm. Thus, after 8 days, the methane production is lower for smaller particle sizes (Figure 4a). This is associated with the decrease in the growth rate of methanogens due to the accumulation of inhibitors. In the same Figure, it can be noted that for particle sizes 550 and 850 µm, the final production is similar. However, a lower slope is observed for the larger particle size, which can be interpreted as a decrease in the growth rate of methanogens due to substrate availability. In Figure 4b, it can be noted that increasing the concentration above 5.6 kg·m^{-3} proportionally manifests the inhibition effect. This was not evident in the simulation at a concentration of 4.6 kg·m^{-3}, suggesting that at this condition, a significant concentration of the inhibitor was not reached.

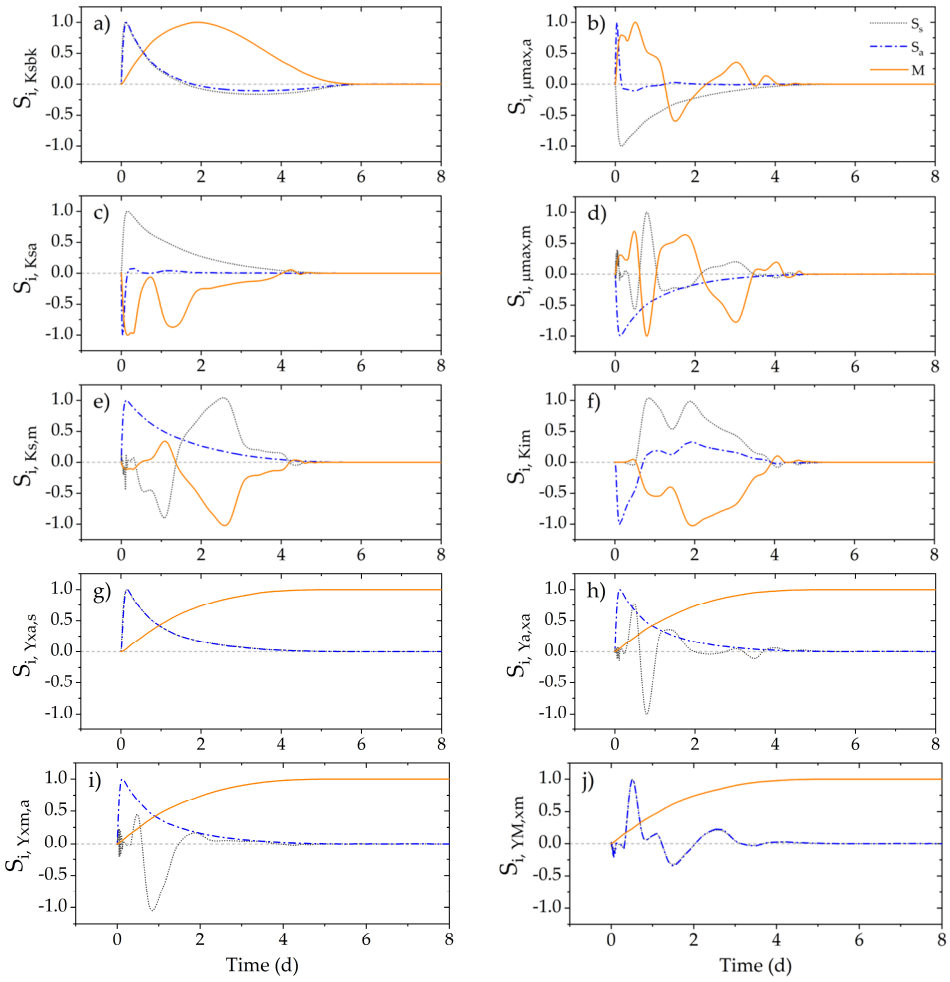


Figure 3. Normalized sensitivity of the *j*-th parameters on soluble substrate (black short dots), volatile fatty acids (blue dashes), and methane (orange solid line). Subplots show the sensitivity of (**a**) K_{sbk}, (**b**) $\mu_{max,a}$, (**c**) K_{sa}, (**d**) $\mu_{max,m}$, (**e**) K_{sm}, (**f**) K_{im}, (**g**) $Y_{x,as}$, (**h**) $Y_{a,xa}$, (**i**) $Y_{x,ma}$, and (**j**) $Y_{M,xm}$.

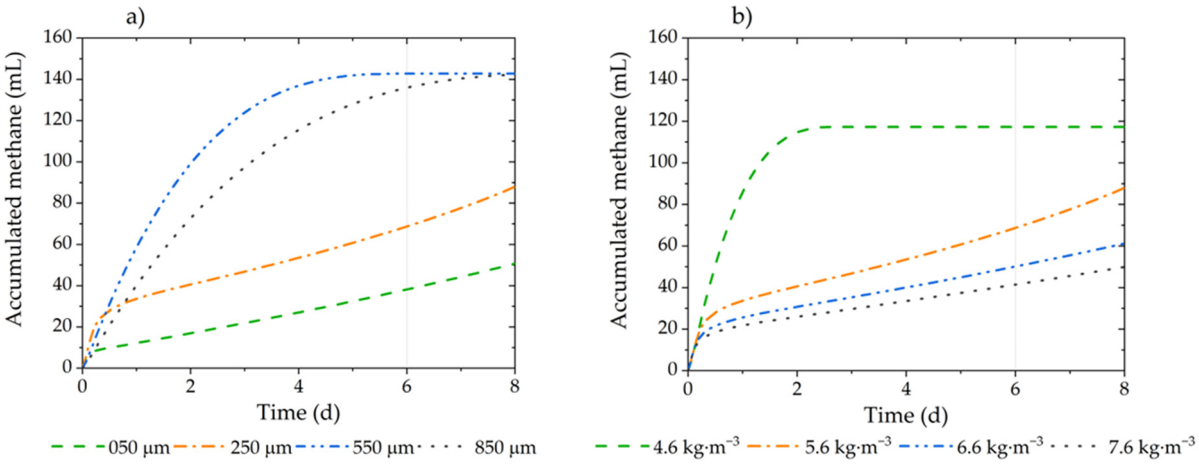


Figure 4. Simulation of accumulated methane production at (**a**) different particle sizes and (**b**) different concentrations of FVW (S_p = 4.6, 5.6, 6.6 and 7.6 kg·m^{-1}).

The correlation between particle size, substrate concentration, and cumulative methane production was established upon the statistical analysis (with α = 0.1) of the simulations proposed in the central composite design of experiments (Table 2). The statistical model determined (Equation (18)) is a quadratic function where the independent variables are

particle size and concentration, and the dependent variable is methane production. This simple model can be useful for directly predicting methane production as a function of the independent variables.

$$M = -460 + 0.671\varnothing + 100S_p - 0.000452\varnothing^2 - 6.1S_p^2 \quad (18)$$

where M represents the accumulated methane (mL), S_p is the substrate concentration (kg·m^3), and $\varnothing$ is the particle size (µm). The determination coefficient of the model was $R^2 = 0.89$, which is acceptable for using as a predictive tool. The constant, linear, and quadratic terms of particle size have a significant effect on methane production with p values of 0.071, 0.040, and 0.087, respectively, with $\alpha = 0.1$ (confidence level of 90%).

The evaluation of Equation (18) results in the response surface and the contour plot shown in Figure 5. It is observed that to increase methane production, the particle size should be reduced to below 900 µm, but if the reduction goes beyond 500 µm, production begins to decrease. This aligns with the premise that the reduction of particle size promotes the release of the available substrate, but excessive reduction leads to the accumulation of inhibitors [14,49,50]. Optimal particle size depends on substrate nature; for example, for food waste with manure, the optimal is 2500 µm [51], while for food waste, the optimal size is >700 µm [15]. In the proposed model, the kinetic parameter that includes this effect is the hydrolysis constant (K_{sbk}); then, for simulation of another type of waste, this parameter should be estimated.

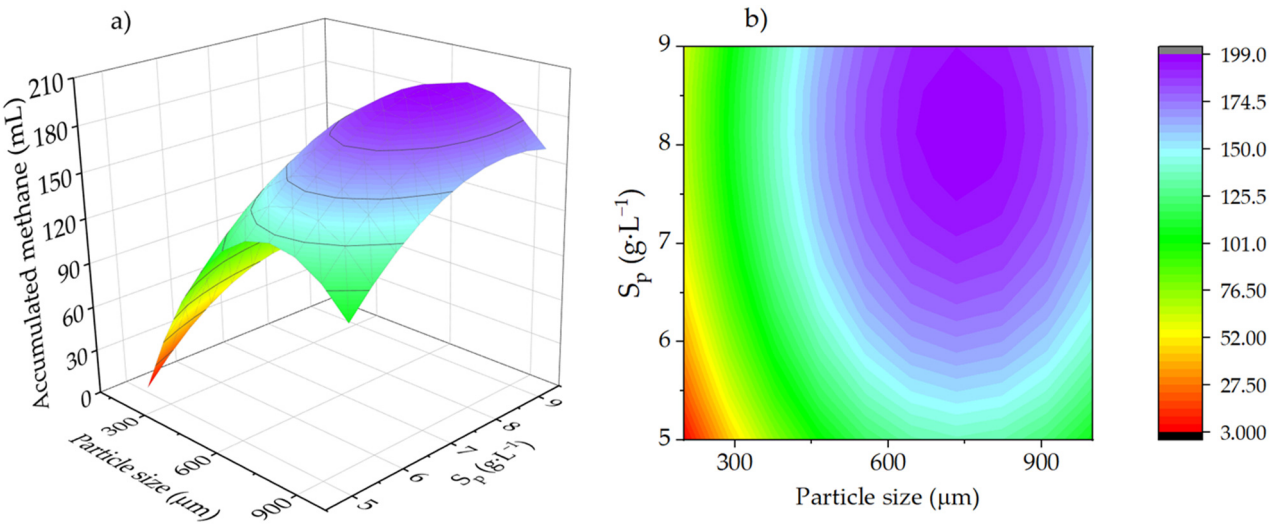


Figure 5. Effect of particle size on anaerobic digestion of fruit and vegetable waste, represented by (**a**) the response surface graph and (**b**) the contour plot.

Finally, the maximum methane production on the response surface (198.9 mL) is observed at a concentration of 8.2 g·L^{-1} with a particle size of 742.3 µm, which corresponds to a methane yield of 303.3 m^3·kg^{-1} VS. This simulated methane yield is consistent with the experimental yield obtained in this study, which ranges from 300.95 to 316.7 m^3·kg^{-1} VS, as well as with results from other studies, where the range is from 131.07 to 560 m^3·kg^{-1} VS. In this range, lower yields have been obtained by digestion of fibrous vegetable waste [52], higher yields for co-digestion of FVW with food waste and manure [51,53], and middle yields (249–355 m^3·kg^{-1} VS) for AD of similar FVW to this study [14,44]. Therefore, the validity of the surface response model can be assumed.

4. Conclusions

This paper analyzed the effect of particle size on methane production from fruit and vegetable waste (FVW). First, experimental assays of FVW with different particle sizes (1.8–1000 µm) in a batch anaerobic digestion (AD) process were performed. Methane yields

ranged from 300 to 316 $m^3 \cdot kg^{-1}$ VS, and process inhibition was observed when digesting particles smaller than 500 µm (yielding 185 $m^3 \cdot kg^{-1}$ VS). Using the experimental data, the parameters of a two-population model with surface-based hydrolysis kinetics were estimated. This model proved to be sensitive to kinetic parameters during the dynamic phase, but stoichiometric parameters that limited methane yield influenced final methane production. By utilizing the simulation results of methane production and applying response surface methodology, a second-order statistical model was established to predict methane production based on particle size and concentration, with a coefficient of determination of 0.89. The optimal conditions determined by the model were a concentration of 8.2 $kg \cdot m^{-3}$ and a particle size of 742.3 µm, with an estimated methane yield of 303.3 $m^3 \cdot kg^{-1}$ VS, consistent with experimental results and the literature. Therefore, the model can be considered valid for simulating the AD of FVW at different particle sizes. Hence, the proposed methodology, which includes simple experimental assays and straightforward phenomenological and statistical models, can be useful for determining the optimal particle size and substrate concentration to improve methane yield in the AD of FVW. For application to other types of residues, it is necessary to estimate the surface-based hydrolysis kinetic constant and adjust the yield coefficients accordingly.

Author Contributions: Conceptualization, J.V., A.V.-P. and H.P.; methodology, J.V.; software, A.V.-P. and R.S.-G.; validation, A.V.-P., R.S.-G. and T.G.-H.; formal analysis, J.V. and H.P.; investigation, G.V.-V. and T.G.-H.; resources, A.V.-P. and H.P.; data curation, J.V., A.V.-P. and H.P.; writing—original draft preparation, J.V.; writing—review and editing, A.V.-P., R.S.-G., T.G.-H., G.V.-V. and H.P.; visualization, R.S.-G., T.G.-H. and G.V.-V.; supervision, A.V.-P. and H.P.; project administration, A.V.-P. All authors have read and agreed to the published version of the manuscript.

Funding: This research received no external funding.

Informed Consent Statement: Not applicable.

Conflicts of Interest: The authors declare no conflicts of interest.

References

1. Sagar, N.A.; Pareek, S.; Sharma, S.; Yahia, E.M.; Lobo, M.G. Fruit and Vegetable Waste: Bioactive Compounds, Their Extraction, and Possible Utilization. *Compr. Rev. Food Sci. Food Saf.* **2018**, *17*, 512–531. [CrossRef] [PubMed]
2. Policastro, G.; Fabbricino, M. Anaerobic Digestion of Food Waste: New Research, Challenges and Opportunities. *Fermentation* **2023**, *9*, 473. [CrossRef]
3. Czekała, W.; Nowak, M.; Bojarski, W. Characteristics of Substrates Used for Biogas Production in Terms of Water Content. *Fermentation* **2023**, *9*, 449. [CrossRef]
4. Usmani, Z.; Sharma, M.; Awasthi, A.K.; Sharma, G.D.; Cysneiros, D.; Nayak, S.C.; Thakur, V.K.; Naidu, R.; Pandey, A.; Gupta, V.K. Minimizing Hazardous Impact of Food Waste in a Circular Economy—Advances in Resource Recovery through Green Strategies. *J. Hazard. Mater.* **2021**, *416*, 126154. [CrossRef]
5. Azevedo, A.; Lapa, N.; Moldão, M.; Duarte, E. Opportunities and Challenges in the Anaerobic Co-Digestion of Municipal Sewage Sludge and Fruit and Vegetable Wastes: A Review. *Energy Nexus* **2023**, *10*, 100202. [CrossRef]
6. Gladchenko, M.A.; Kovalev, D.A.; Kovalev, A.A.; Litti, Y.V.; Nozhevnikova, A.N. Methane Production by Anaerobic Digestion of Organic Waste from Vegetable Processing Facilities. *Appl. Biochem. Microbiol.* **2017**, *53*, 242–249. [CrossRef]
7. Mata-Alvarez, J. *Biomethanization of Organic Fraction of Municipal Solid Wastes*; IWA Publishing: Cornwall, UK, 2002.
8. Mata-Alvarez, J.; Macé, S.; Llabrés, P. Anaerobic Digestion of Organic Solid Wastes. An Overview of Research Achievements and Perspectives. *Bioresour. Technol.* **2000**, *74*, 3–16. [CrossRef]
9. Xu, F.; Li, Y.; Ge, X.; Yang, L.; Li, Y. Anaerobic Digestion of Food Waste—Challenges and Opportunities. *Bioresour. Technol.* **2018**, *247*, 1047–1058. [CrossRef]
10. Liu, K.; Lv, L.; Li, W.; Ren, Z.; Wang, P.; Liu, X.; Gao, W.; Sun, L.; Zhang, G. A Comprehensive Review on Food Waste Anaerobic Co-Digestion: Research Progress and Tendencies. *Sci. Total Environ.* **2023**, *878*, 163155. [CrossRef]
11. Terashima, M.; Goel, R.; Komatsu, K.; Yasui, H.; Takahashi, H.; Li, Y.Y.; Noike, T. CFD Simulation of Mixing in Anaerobic Digesters. *Bioresour. Technol.* **2009**, *100*, 2228–2233. [CrossRef]
12. Zhang, Y.; Banks, C.J. Impact of Different Particle Size Distributions on Anaerobic Digestion of the Organic Fraction of Municipal Solid Waste. *Waste Manag.* **2013**, *33*, 297–307. [CrossRef] [PubMed]
13. Sanders, W.T.M.; Geerink, M.; Zeeman, G.; Lettinga, G. Anaerobic Hydrolysis Kinetics of Particulate Substrates. *Water Sci. Technol.* **2000**, *41*, 17–24. [CrossRef] [PubMed]

14. Zia, M.; Ahmed, S.; Kumar, A. Anaerobic Digestion (AD) of Fruit and Vegetable Market Waste (FVMW): Potential of FVMW, Bioreactor Performance, Co-Substrates, and Pre-Treatment Techniques. *Biomass Convers. Biorefin.* **2022**, *12*, 3573–3592. [CrossRef]
15. Izumi, K.; Okishio, Y.K.; Nagao, N.; Niwa, C.; Yamamoto, S.; Toda, T. Effects of Particle Size on Anaerobic Digestion of Food Waste. *Int. Biodeterior. Biodegrad.* **2010**, *64*, 601–608. [CrossRef]
16. Edwiges, T.; Frare, L.M.; Lima Alino, J.H.; Triolo, J.M.; Flotats, X.; Silva de Mendonça Costa, M.S. Methane Potential of Fruit and Vegetable Waste: An Evaluation of the Semi-Continuous Anaerobic Mono-Digestion. *Environ. Technol.* **2020**, *41*, 921–930. [CrossRef]
17. Ganesh, R.; Torrijos, M.; Sousbie, P.; Lugardon, A.; Steyer, J.P.; Delgenes, J.P. Single-Phase and Two-Phase Anaerobic Digestion of Fruit and Vegetable Waste: Comparison of Start-up, Reactor Stability and Process Performance. *Waste Manag.* **2014**, *34*, 875–885. [CrossRef]
18. Magama, P.; Chiyanzu, I.; Mulopo, J. A systematic review of sustainable fruit and vegetable waste recycling alternatives and possibilities for anaerobic biorefinery. *Bioresour. Technol. Rep.* **2022**, *18*, 101031. [CrossRef]
19. Kratky, L.; Jirout, T. Biomass size reduction machines for enhancing biogas production. *Chem. Eng. Technol.* **2011**, *34*, 391–399. [CrossRef]
20. Ganeshan, P.; Rajendran, K. Dynamic Simulation and Optimization of Anaerobic Digestion Processes Using MATLAB. *Bioresour. Technol.* **2022**, *351*, 126970. [CrossRef]
21. Donoso-Bravo, A.; Mailier, J.; Martin, C.; Rodríguez, J.; Aceves-Lara, C.A.; Wouwer, A. Vande Model Selection, Identification and Validation in Anaerobic Digestion: A Review. *Water Res.* **2011**, *45*, 5347–5364. [CrossRef]
22. Graef, S.P.; Andrews, J.F. Mathematical Modeling and Control of Anaerobic Digestion. *Water Res.* **1974**, *8*, 261–289.
23. Hill, D.T.; Barth, C.L. A Dynamic Model for Simulation of Animal Waste Digestion. *J. Water Pollut. Control Fed.* **1977**, *49*, 2129–2143.
24. Emebu, S.; Pecha, J.; Janáčová, D. Review on Anaerobic Digestion Models: Model Classification & Elaboration of Process Phenomena. *Renew. Sustain. Energy Rev.* **2022**, *160*, 112288. [CrossRef]
25. Batstone, D.J.; Keller, J.; Angelidaki, I.; Kalyuzhnyi, S.V.; Pavlostathis, S.G.; Rozzi, A.; Sanders, W.T.; Siegrist, H.; Vavilin, V.A. The IWA Anaerobic Digestion Model No 1 (ADM1). *Water Sci. Technol.* **2002**, *45*, 65–73. [CrossRef]
26. Batstone, D.J.; Puyol, D.; Flores-Alsina, X.; Rodríguez, J. Mathematical Modelling of Anaerobic Digestion Processes: Applications and Future Needs. *Rev. Environ. Sci. Biotechnol.* **2015**, *14*, 595–613. [CrossRef]
27. Zhao, X.; Li, L.; Wu, D.; Xiao, T.; Ma, Y.; Peng, X. Modified Anaerobic Digestion Model No. 1 for Modeling Methane Production from Food Waste in Batch and Semi-Continuous Anaerobic Digestions. *Bioresour. Technol.* **2019**, *271*, 109–117. [CrossRef]
28. Weinrich, S.; Mauky, E.; Schmidt, T.; Krebs, C.; Liebetrau, J.; Nelles, M. Systematic Simplification of the Anaerobic Digestion Model No. 1 (ADM1)—Laboratory Experiments and Model Application. *Bioresour. Technol.* **2021**, *333*, 125104. [CrossRef]
29. Weinrich, S.; Nelles, M. Systematic Simplification of the Anaerobic Digestion Model No. 1 (ADM1)—Model Development and Stoichiometric Analysis. *Bioresour. Technol.* **2021**, *333*, 125124. [CrossRef]
30. Fernández, L.C. *Manual de Técnicas de Análisis de Suelos Aplicadas a La Remediación de Sitios Contaminados*; Instituto Mexicano del Petroleo, Secretaría de Medio Ambiente y Recursos Naturales: Mexico City, Mexico, 2006.
31. Eaton, A.D.; Clesceri, L.S.; Greenberg, A.E. *Standard Methods for the Examination of Water and Wastewater*, 19th ed.; American Public Health Association: Washington, DC, USA, 1998.
32. *NMX-AA-026-SCFI-2001*; Water Analysis—Determination of Total Kjeldahl Nitrogen in Natural Water, Wastewaters and Treated Water—Test Method. Secretaria de Energía: Ciudad de México, Mexico, 2001.
33. Rabii, A.; El Sayed, A.; Ismail, A.; Aldin, S.; Dahman, Y.; Elbeshbishy, E. Optimizing the Mixing Ratios of Source-Separated Organic Waste and Thickened Waste Activated Sludge in Anaerobic Co-Digestion: A New Approach. *Processes* **2024**, *12*, 794. [CrossRef]
34. Field, J.A. Limits of Anaerobic Biodegradation. *Water Sci. Technol.* **2002**, *45*, 9–18. [CrossRef]
35. Esposito, G. Bio-Methane Potential Tests to Measure the Biogas Production from the Digestion and Co-Digestion of Complex Organic Substrates. *Open Environ. Eng. J.* **2012**, *5*, 1–8. [CrossRef]
36. Kiely, G.; Tayfur, G.; Dolan, C.; Tanji, K. Physical and Mathematical Modelling of Anaerobic Digestion of Organic Wastes. *Water Res.* **1997**, *31*, 534–540. [CrossRef]
37. Monod, J. The Growth of Bacterial Cultures. *Annu. Rev. Microbiol.* **1949**, *3*, 371–394. [CrossRef]
38. Andrews, J.F. Dynamic Model of the Anaerobic Digestion Process. *J. Sanit. Eng. Div.* **1969**, *95*, 95–116. [CrossRef]
39. Moletta, R.; Verrier, D.; Albagnac, G. Dynamic Modelling of Anaerobic Digestion. *Water Res.* **1986**, *20*, 427–434. [CrossRef]
40. Tartakovsky, B.; Mu, S.J.; Zeng, Y.; Lou, S.J.; Guiot, S.R.; Wu, P. Anaerobic Digestion Model No. 1-Based Distributed Parameter Model of an Anaerobic Reactor: II. Model Validation. *Bioresour. Technol.* **2008**, *99*, 3676–3684. [CrossRef]
41. Mathur, R.; Sharma, M.K.; Loganathan, K.; Abbas, M.; Hussain, S.; Kataria, G.; Alqahtani, M.S.; Srinivas Rao, K. Modeling of Two-Stage Anaerobic Onsite Wastewater Sanitation System to Predict Effluent Soluble Chemical Oxygen Demand through Machine Learning. *Sci. Rep.* **2024**, *14*, 1835. [CrossRef]
42. Montgomery, D.C. *Design and Analysis of Experiments*; John Wiley & Sons: Hoboken, NJ, USA, 2017.
43. Edwiges, T.; Frare, L.; Mayer, B.; Lins, L.; Mi Triolo, J.; Flotats, X.; de Mendonça Costa, M.S.S. Influence of Chemical Composition on Biochemical Methane Potential of Fruit and Vegetable Waste. *Waste Manag.* **2018**, *71*, 618–625. [CrossRef]
44. Ji, C.; Kong, C.X.; Mei, Z.L.; Li, J. A Review of the Anaerobic Digestion of Fruit and Vegetable Waste. *Appl. Biochem. Biotechnol.* **2017**, *183*, 906–922. [CrossRef]

45. Zeshan, K.; Karthikeyan, O.P.; Visvanathan, C. Effect of C/N Ratio and Ammonia-N Accumulation in a Pilot-Scale Thermophilic Dry Anaerobic Digester. *Bioresour. Technol.* **2012**, *113*, 294–302. [CrossRef]
46. Vigueras-Carmona, S.E.; Ramírez, F.; Noyola, A.; Monroy, O. Effect of Thermal Alkaline Pretreatment on the Anaerobic Digestion of Wasted Activated Sludge. *Water Sci. Technol.* **2011**, *64*, 953–959. [CrossRef] [PubMed]
47. De Pauw, D.J.W.; Vanrolleghem, P.A. Practical Aspects of Sensitivity Function Approximation for Dynamic Models. *Math. Comput. Model. Dyn. Syst.* **2006**, *12*, 395–414. [CrossRef]
48. Martínez, E.J.; González, R.; Ellacuriaga, M.; Gómez, X. Valorization of Fourth-Range Wastes: Evaluating Pyrolytic Behavior of Fresh and Digested Wastes. *Fermentation* **2022**, *8*, 744. [CrossRef]
49. Liu, W.-Y.; Liao, B. Anaerobic Co-Digestion of Vegetable and Fruit Market Waste in LBR + CSTR Two-Stage Process for Waste Reduction and Biogas Production. *Appl. Biochem. Biotechnol.* **2019**, *188*, 185–193. [CrossRef]
50. Morales-Polo, C.; del Mar Cledera-Castro, M.; Moratilla Soria, B.Y. Reviewing the Anaerobic Digestion of Food Waste: From Waste Generation and Anaerobic Process to Its Perspectives. *Appl. Sci.* **2018**, *8*, 1804. [CrossRef]
51. Agyeman, F.O.; Tao, W. Anaerobic Co-Digestion of Food Waste and Dairy Manure: Effects Offood Waste Particle Size and Organic Loading Rate. *J. Environ. Manag.* **2014**, *133*, 268–274. [CrossRef]
52. Czubaszek, R.; Wysocka-Czubaszek, A.; Tyborowski, R. Methane Production Potential from Apple Pomace, Cabbage Leaves, Pumpkin Residue and Walnut Husks. *Appl. Sci.* **2022**, *12*, 6128. [CrossRef]
53. Agrawal, A.V.; Chaudhari, P.K.; Ghosh, P. Effect of Mixing Ratio on Biomethane Potential of Anaerobic Co-Digestion of Fruit and Vegetable Waste and Food Waste. *Biomass Convers. Biorefin.* **2023**, *14*, 16149–16158. [CrossRef]

Disclaimer/Publisher's Note: The statements, opinions and data contained in all publications are solely those of the individual author(s) and contributor(s) and not of MDPI and/or the editor(s). MDPI and/or the editor(s) disclaim responsibility for any injury to people or property resulting from any ideas, methods, instructions or products referred to in the content.